Bull. Mater. Sci., Vol. 37, No. 7, December 2014, pp. 1663–1668. © Indian Academy of Sciences.

Influence of growth temperature on morphological, structural and photoluminescence properties of ZnO nanostructure thin layers and powders deposited by thermal evaporation

YASER ARJMAND and HOSEIN ESHGHI*
Department of Physics, University of Shahrood, Shahrood 36155-316, Iran

MS received 9 April 2013; revised 13 January 2014

Abstract. **Zinc oxide (ZnO) nanostructures were grown as thin films on the p-silicon (100) wafer and also in the form of powder inside the boat by heating (550–950 °C) zinc powder in the presence of oxygen without any catalyst or additives, using the thermal evaporation method. The field-emission scanning electron microscopy images, as well as energy-dispersive X-ray spectroscopy and X-ray diffraction spectra, indicate that although the grown samples are covered with various nanostructure shapes, such as nanowires, nanorods, flower-like nanostructures and microcages, all have a reasonable stoichiometric composition in the polycrystalline wurtzite phase along (002) in the thin layer samples and along (101) in the powder samples within the boat. The room-temperature photoluminescence spectra of the thin layer samples revealed not only the ultraviolet (UV) emission blue shift of the samples with an increase in the growth temperature, but also found that the emission intensity ratio of UV/visible (∼510 nm) has a maximum and minimum, corresponding to that grown at 750 and 950 °C, respectively.**

Keywords. **ZnO; thin film; nanocrystalline material; thermal evaporation; photoluminescence.**

1. Introduction

With the emergence of nanoscience and nanotechnology, semiconductor nanomaterials such as nanotubes, nanorods, nanowires and nanobelts have received much attention due to their unique and novel properties, when compared with bulk materials (Tang and Kotov 2005; Comini *et al* 2009). Among the already known semiconductor nanomaterials, zinc oxide (ZnO) has a number of important advantages: firstly, it is a semiconductor with a direct wide bandgap of 3·37 eV and a large excitation binding energy (∼60 meV) which make it an important functional oxide, exhibiting near-ultraviolet (UV) emission and transparent conductivity at room temperature and higher temperature (Wang 2007). Secondly, it is a piezoelectric material due to the non-central crystalline symmetry. This is a key phenomenon in building electro-mechanical coupled sensors and transducers at nanoscale sizes. It is found that the piezoelectric coefficient in nanobelt shape samples is about three times more than that of its bulk ones (Zhao *et al* 2004). Thirdly, ZnO is a biocompatible material which makes it useful for biochemical and biomedical applications (Nie *et al* 2006). Finally, it is a promising material for various electronics and optoelectronics purposes including solar cells (Baxtera and Aydil 2006), gas sensors (Oh *et al* 2009), optoelectronic devices (Suehiro *et al* 2006), field-emission devices (Wei *et al* 2007a), light-emitting diodes (Guo *et al* 2009), etc. ZnO nanostructures have been synthesized by various methods such as thermal evaporation (Abdulgafour *et al* 2010), sol–gel (Li *et al* 2008), metal organic chemical vapour deposition (Kar *et al* 2010), spray pyrolysis (Dedova *et al* 2007), pulsed laser deposition (Chen *et al* 2005), etc. The growth temperature is one of the key parameters which ought to be considered before employing ZnO nanostructures in various applications. A number of research groups have studied the dependency of the growth temperature on the morphology and luminescence properties of the ZnO nanostructures (Fang *et al* 2008; Al-Azri *et al* 2010; Yousefi *et al* 2011). They have used a mixture of ZnO and graphite powders in their experiments at source temperatures above 950 °C in order to study the influence of this parameter on the morphological and optical properties of ZnO nanostructures. Hou *et al* (2009) have studied the effect of synthesis temperature on the morphologies and field-emission properties of ZnO nanostructures fabricated by heating zinc (Zn) powder in the presence of oxygen on the silicon (Si) substrate coated with 2 μm gold as the catalyst.

In the present study, ZnO nanostructures are deposited on the p-Si (100) wafer by heating Zn powder in the presence of oxygen gas without any catalyst or additives, using the thermal evaporation method at various temperatures. In addition to these samples, we have simultaneously characterized the powder samples rested in the boat.

2. Experimental

ZnO nanostructures were fabricated on the p-type Si (100) substrate and simultaneously within the boat in the temperature range of 550–950 °C by the thermal evaporation method,

*Author for correspondence (h_eshghi@shahroodut.ac.ir)

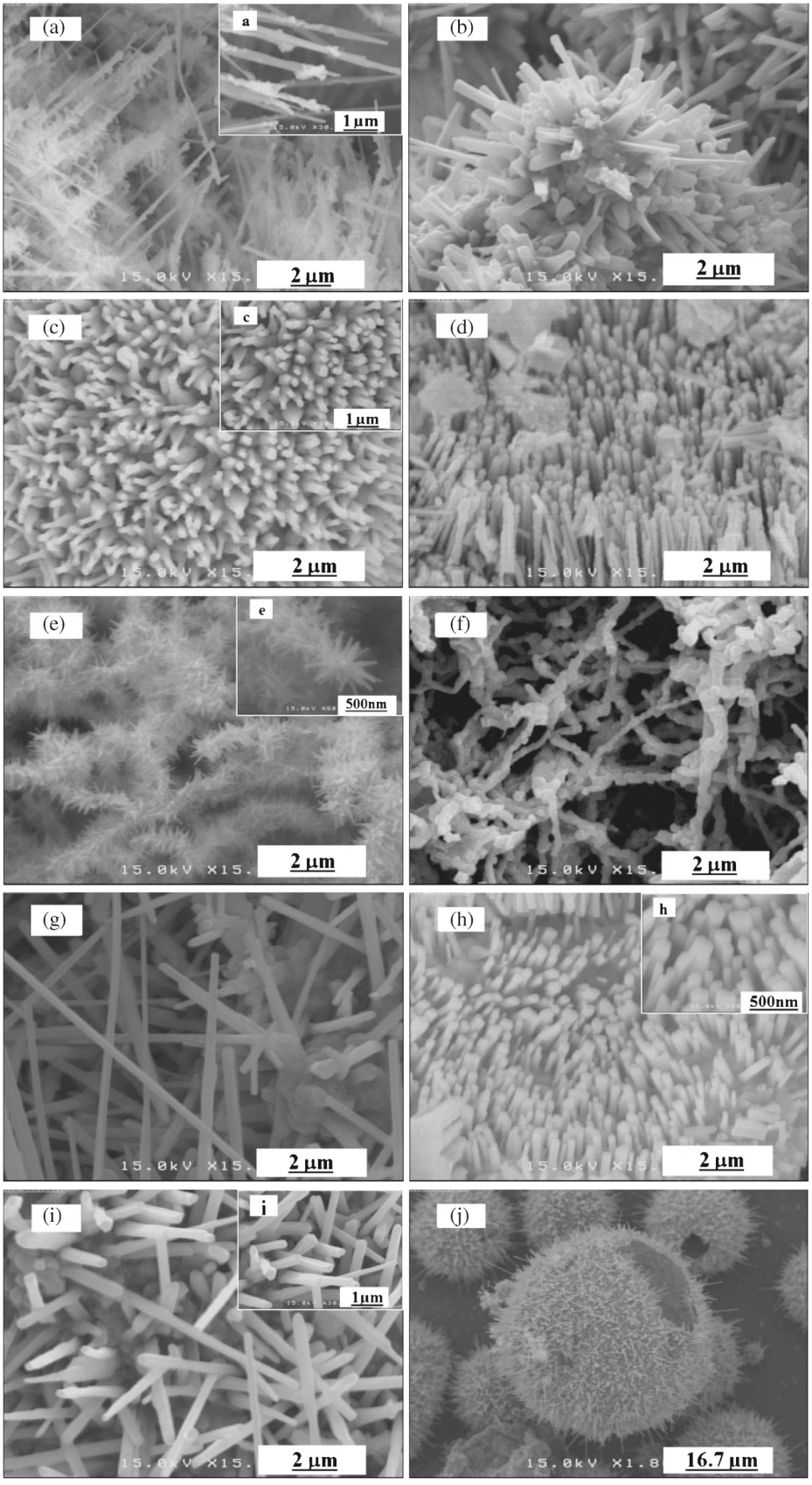

Figure 1. FESEM images of synthesized ZnO nanostructures: (**a**), (**c**), (**e**), (**g**) and (**i**) for samples grown on the Si substrate; and (**b**), (**d**), (**f**), (**h**) and (**j**) for those inside the boat, at 550, 650, 750, 850 and 950 °C, respectively.

using a horizontal quartz tube furnace. In this research, Zn powder (Alfa Aesar, 99·9%) and oxygen gas were used as the constituent materials. During the growth process of each sample, Zn powder (about 2 g) was placed in a quartz boat located at the centre of the horizontal furnace. In our experiments, the Si substrates were located 10 cm from source material. It is notable that both the boat and the substrate were held at the same temperature. After arrangement of the samples, the tube was evacuated with a pressure of 10^{-4} Torr. During each growth temperature, the furnace was heated with a heating rate of 10 °C/min under a constant flow of argon as a carrier gas with the flow rate of 300 sccm. When the furnace temperature reached an appropriate temperature, oxygen as a reactant gas was introduced into it for 80 min at a flow rate of 100 sccm. Eventually, the furnace was cooled down to room temperature and the product, in the boat and on the surface of the Si substrate was extracted.

The morphology of the synthesized samples was examined using the field-emission scanning electron microscopy (FESEM, Hitachi S-4160). The phase and crystallinity of the samples were studied by the X-ray diffraction (XRD, Bruker-AXS) system, using Cu-K_α radiation ($\lambda = 1{\cdot}5404$ Å). Energy-dispersive X-ray spectroscopy (EDS TESCAN VEGA) was used to determine the chemical composition of the deposited material, and the optical characterization of the samples was performed by a fluorescence spectrophotometer, using a Xe lamp with an excitation wavelength of 325 nm at room temperature.

3. Results and discussion

3.1 *Surface morphology and EDS data*

Figure 1 shows the surface morphology of the ZnO nanostructures deposited on the Si substrate as a thin layer as well as the ZnO powder samples rested in the boat at various temperatures of 550, 650, 750, 850 and 950 °C. According to these images, the thin grown sample at 550 °C (figure 1a) consists of compact branched nanowires. As it is clear, the wires are not completely smooth and are included with some dispersed nanodendrites. Figure 1(b) shows the surface morphology of the remainder ZnO powder in the boat at the same temperature consisting of nanowires. As the temperature is increased to 650 °C, both the thin layer and the powder sample (figure 1c and d) are occupied by the compact area of aligned ZnO nanorods. In turn, figure 1(e) shows flower-like ZnO nanostructures on the Si substrate, at 750 °C, with hexagonal crowns on the branches of these structures. Meanwhile, figure 1(f) shows that the generated sample in the boat at the same temperature consists of entangled nanowires. At 850 °C, the formation of ZnO sprawled nanowires was synthesized on the Si substrate (figure 1g) and also nanorods with hexagonal cross section in the boat (figure 1h). The synthesized sample at 950 °C exhibits more uniform size distribution of rod-like shapes on the Si substrate (figure 1i) than those grown at 850 °C, and in sphere-like hollow microcage shapes and rough surface covered with very thin nanowire in the boat (figure 1j). All these images reflect the fact that the surface morphology of ZnO nanostructures is very sensitive to the growth temperature and also the position of the sample. Table 1 briefly shows the average sizes (diameter and length) of the synthesized nanostructures.

To figure out the purity of the grown samples, we performed the EDS experiment on sample i, figure 2. According to the quantitative data (Zn: 51 at%, O: 43 at% and Si: 6 at%), although the layer suffers the lack of oxygen atoms thus deviating from a perfect stoichiometric composition it confirms the purity of the sample from alien atoms.

3.2 *Structural analysis*

The XRD spectrum is used to obtain information about crystallinity and the crystal phases of the grown products. Figure 3(a) and (b) shows the XRD spectra of the samples synthesized on the Si substrate and the powder inside the boat, respectively. The results indicate a polycrystalline wurtzite structure in all samples. It is noted that the deposited layers on the Si substrate are mainly grown along the (002) planes, while the powder samples in the boat are preferred to grow almost along (101). Moreover, as it is clear from the results, in the thin layer samples, the intensity of the (002) peak has increased by increasing the growth temperature and has reached a maximum at 950 °C, while in the powder samples the (101) peak has a maximum intensity at 550 °C and tend to a minimum at 950 °C.

Knowing Bragg's diffraction angle (θ) as well as the full-width at half-maximum (β) in the predominant peak

Table 1. Estimated diameters of the fabricated ZnO nanostructures.

Growth temperature (°C)	Thin layer samples		Powder samples	
	Diameter (nm)	Length (μm)	Diameter (nm)	Length (μm)
550	100	Several	100–200	1–2
650	100	100	100–200	1·5
750	50	0·3	100–200	Several
850	100–200	Several	70–200	$\sim$ 0·5
950	100	100–200	Microcages: $\sim$ 50 μm	Fine N-wire coverage

of these spectra, it is possible to calculate the lattice constants (a and c) using the below relation (Cullity and Stock 2001)

$$\frac{1}{d^2_{(hkl)}} = \frac{4}{3}\left[\frac{h^2+hk+k^2}{a^2}\right] + \frac{l^2}{c^2}$$

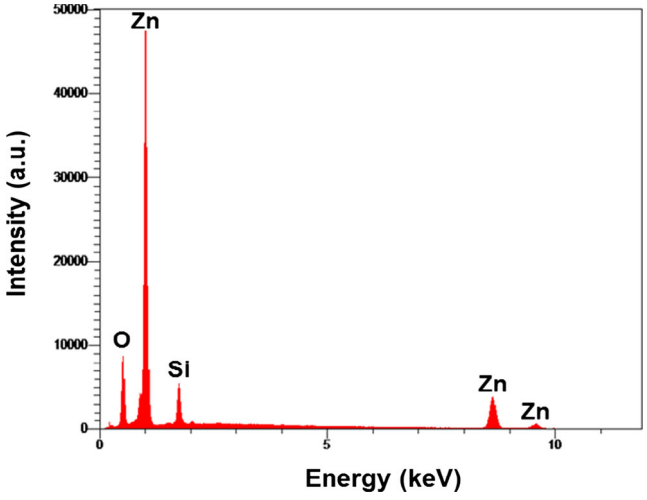

Figure 2. EDS spectrum of ZnO layer (sample i).

and the crystallite size (D) of these structures using Scherrer's formula (Ibrahim *et al* 2004)

$$D = \frac{0{\cdot}9\lambda}{\beta\cos\theta},$$

where λ is the X-ray wavelength. In addition to the above parameters the strain of the layers could also be calculated using the relation (Sawaby *et al* 2010)

$$\varepsilon = \beta\cos\theta/4.$$

The calculated values are presented in table 2. As it is evident, not only the crystallite sizes but also the lattice constants and the induced strains of these samples are sensitive to the substrate temperature.

3.3 *Photoluminescence (PL) spectra*

The PL spectrum of a material is a reliable method in accurately studying the band structure and the position of the localized states therein. Figure 4 shows the results of these measurements for the ZnO nanostructures grown on the Si substrate. In these spectra, two instinctive main emissions are present: (1) an intrinsic UV emission, which is related to the recombination of free excitons through an

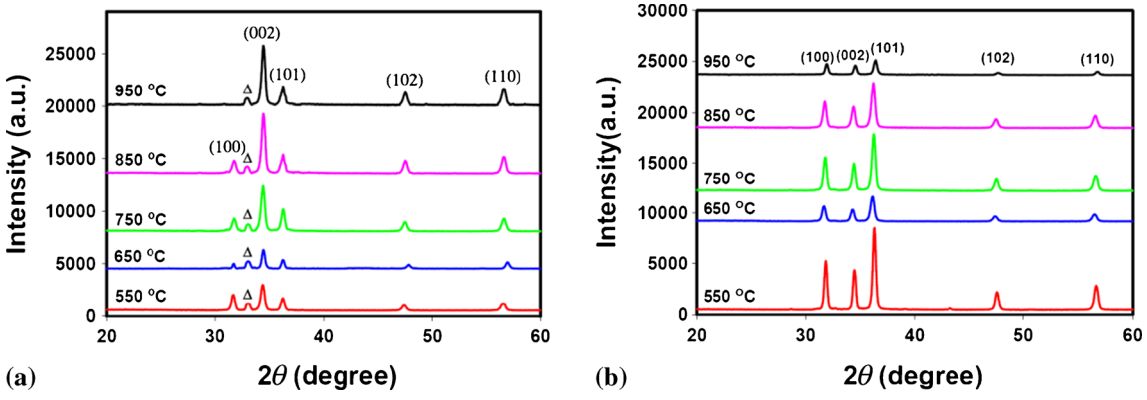

Figure 3. XRD patterns of the ZnO nanostructures grown at different temperatures: (**a**) samples deposited on the Si substrate (the Δ assigned peaks are related to the Si substrate itself) and (**b**) the corresponding ZnO powders in the boat.

Table 2. The lattice constants, crystallite sizes and the induced strains of the two groups of samples. According to standard data reports in JCPDS card (no. 36-1451) in bulk ZnO wurtzite structure: $a = 3{\cdot}249$ Å, $c = 5{\cdot}206$ Å.

Growth Temperature (°C)	Thin layer samples				Powder samples			
	a (Å)	c (Å)	D (nm)	ε ($\times 10^{-3}$)	a (Å)	c (Å)	D (nm)	ε ($\times 10^{-3}$)
550	3·258	5·216	24·5	1·41	3·241	5·193	31·0	1·12
650	3·255	5·209	30·0	1·17	3·256	5·202	24·6	1·43
750	3·253	5·219	24·2	1·40	3·246	5·226	26·1	1·32
850	3·241	5·221	26·5	1·30	3·251	5·198	25·6	1·43
950	3·246	5·213	25·4	1·32	3·242	5·178	27·9	1·24

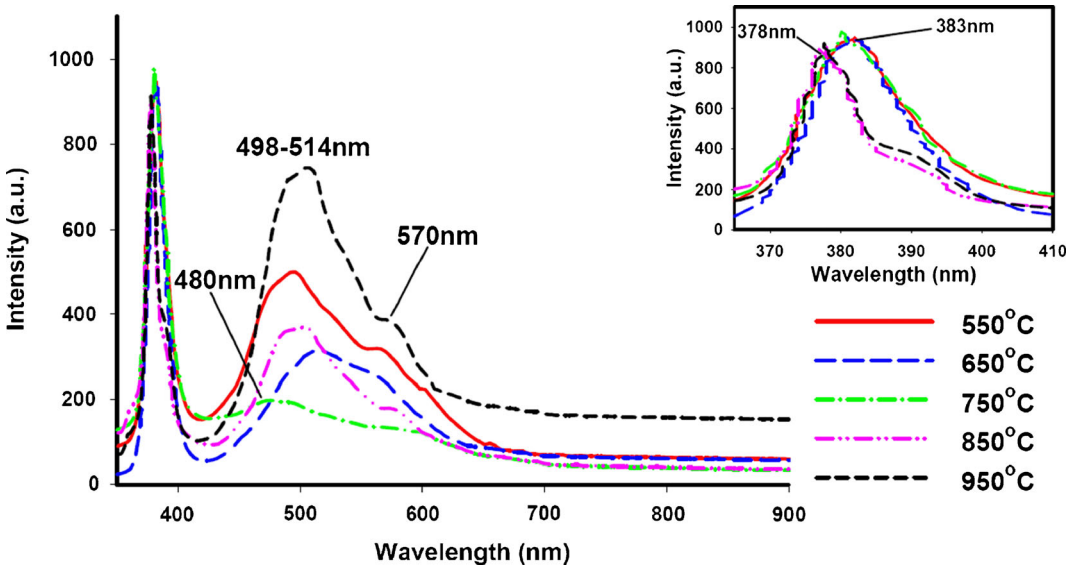

Figure 4. Room temperature PL spectra of ZnO nanostructure deposited on the Si substrate at various temperatures. The inset shows the UV peak blue shift by increments in the substrate temperature, with some irregularities as a result of the presence of induced strains in the material.

exciton–exciton collision process between conduction and valence bands (Kong *et al* 2001; Umar and Hahn 2006). As it is evident from the inset, this peak emission is gradually shifted towards lower wavelengths, i.e. from 383 nm (3·24 eV) for the sample grown at 550 °C to 378 nm (3·29 eV) for the one grown at 950 °C, with some irregularities, could be related to the induced strains in the films, table 2 (Li *et al* 2008); (2) a series of broad visible peaks centred around 480 nm (2·6 eV), 498–514 nm (2·42–2·49 eV) and 570 nm (2·18 eV) corresponding to blue, green and yellow colors, respectively. The blue emission is ascribed to the electronic transition from the donor energy level of Zn interstitials to the acceptor energy levels of Zn vacancies (Wei *et al* 2007b). The green luminescence is attributed to the antisite oxygen atoms (Lin *et al* 2001) and the yellow emission is commonly attributed to the interstitial oxygen defects (Kwok *et al* 2006; Li *et al* 2008). From these spectra, one can infer that the intensity ratio of the UV to visible emission is maximum for the sample grown at 750 °C and minimum for the one grown at 950 °C.

4. Conclusions

In this report, we have investigated the surface morphology, EDS, XRD and PL spectra of the ZnO nanostructure samples prepared by thermal evaporation of metallic Zn powder in the temperature range of 550–950 °C on the Si substrate and also inside the boat itself. The surface morphology and EDS data represent the formation of various nanostructures, although pure, with few atomic percentages of oxygen deficiencies. The XRD spectra revealed the existence of thepolycrystalline wurtzite structure in all samples with the preferred orientations of (002) and (101) in the thin layer and powder samples, respectively. The PL spectra of the thin layers showed that: as the growth temperature is increased a blue shift in the intrinsic UV emission occurred as a result of various morphologies, crystallite sizes and induced strains; and the intensity ratio of UV to visible emission becomes maximum for the grown sample at 750 °C and minimum for the one grown at 950 °C.

References

Abdulgafour H I, Hassan Z, Al-Hardan N and Yam F K 2010 *Physica B* **405** 2570

Al-Azri K, Nor R M, Amin Y M and Al-Ruqeishi M S 2010 *Appl. Surf. Sci.* **256** 5957

Baxtera J B and Aydil E S 2006 *Sol. Energy Mater. Sol. Cells* **90** 607

Chen J J, Yu M H, Zhou W L, Sun K and Wang L M 2005 *Appl. Phys. Lett.* **87** 173119

Comini E, Baratto C, Faglia G, Ferroni M, Vomiero A and Sberveglieri G 2009 *Prog. Mater. Sci.* **1** 54

Cullity B D and Stock S R 2001 *Elements of X-ray diffraction* (New Jersey, USA: Prentice Hall) 3rd edn, p 619

Dedova T, Volobujeva O, Klauson J, Mere A and Krunks M 2007 *Nanoscale Res. Lett.* **2** 391

Fang F, Zhao D X, Zhang J Y, Shen D Z, Lu Y M, Fan X W, Li B H and Wang X H 2008 *Mater. Lett.* **62** 1092

Guo R, Nishimura J, Matsumoto M, Higashihata M, Nakamura D and Okada T 2009 *Appl. Phys. B* **94** 33

Hou K, Li C, Lei W, Zhang X, Yang X, Qu K, Wang B, Zhao Z and Sun X W 2009 *Physica E* **41** 470

Ibrahim A A, El-Sayed N Z, Kaid M A and Ashour A 2004 *Vacuum* **5** 189

Kar J P, Das S N, Choi J H, Lee T I and Myoung J M 2010 *Appl. Surf. Sci.* **256** 4995

Kong Y C, Yu D P, Zhang B, Fang W and Feng S Q 2001 *Appl. Phys. Lett.* **78** 407

Kwok W M, Djurišič A B, Leung Y H, Li D, Tam K H, Phillips D L and Chan W K 2006 *Appl. Phys. Lett.* **89** 183112

Li J, Srinivasan S, He G N, Kang J Y, Wu S T and Ponce F A 2008 *J. Cryst. Growth* **310** 599

Lin B, Fu Z and Jia Y 2001 *Appl. Phys. Lett.* **79** 943

Nie L, Gao L, Feng P, Zhang J, Fu X, Liu Y, Yan X and Wang T 2006 *Small* **2** 621

Oh E, Choi H Y, Jung S H, Cho S, Kim J C, Lee K H, Kang S W, Kim J, Yun J Y and Jeong S H 2009 *Sens. Actuators B: Chem.* **141** 239

Sawaby A, Selim M S, Marzouk S Y, Mostafa M A and Hosny A 2010 *Physica B* **405** 3412

Suehiro J, Nakagawa N, Hidaka S I, Ueda M, Imasaka K, Higashihata M, Okada T and Hara M 2006 *Nanotechnology* **17** 2567

Tang Z and Kotov N A 2005 *Adv. Mater.* **17** 951

Umar A and Hahn Y B 2006 *Nanotechnology* **17** 2174

Wang Z L 2007 *Appl. Phys. A* **88** 7

Wei L, Zhang X and Zuoya Z 2007a *J. Vac. Sci. Technol. B* **25** 608

Wei X Q, Man B Y, Liu M, Xue C S, Zhuang H Z and Yang C 2007b *Physica B* **388** 145

Yousefi R, Muhamad M R and Zak A K 2011 *Curr. Appl. Phys.* **11** 767

Zhao M H, Wang Z L and Mao S X 2004 *Nano Lett.* **4** 587